

# **INTERFERENCE MITIGATION AND CHANNEL EQUALIZATION FOR ARTM TIER-1 WAVEFORMS USING KALMAN FILTER**

**Otilia Popescu, Mohammad Saquib**

**Dept. Electrical Engineering, University of Texas at Dallas, Richardson, TX**

**Dimitrie C. Popescu**

**Dept. Electrical & Computer Engineering, University of Texas at San Antonio**

**Michael Rice**

**Dept. Electrical & Computer Engineering, Brigham Young University, Provo, UT**

## **ABSTRACT**

In this paper we describe a new method that is applicable to mitigating both multipath interference and adjacent channel interference (ACI) in aeronautical telemetry applications using ARTM Tier-1 waveforms. The proposed method uses a linear equalizer that is derived using Kalman filtering theory, which has been used for channel equalization for high-speed communication systems. We illustrate the proposed method with numerical examples obtained from simulations that show the bit error rate performance (BER) for different modulation schemes.

## **KEY WORDS**

Interference mitigation, channel equalization, Kalman filter, adjacent channel interference, FQPSK, SOQPSK

## **INTRODUCTION**

Data rates required in modern aeronautical telemetry applications have increased, thus generating more demand for bandwidth for telemetry signals. As a consequence new modulation schemes with improved spectral efficiency have been proposed for use in aeronautical telemetry. Among these we note the Feher-patented QPSK modulation (FQPSK) [1] and the Shaped-Offset QPSK

modulation (SOQPSK) [2] also known as Advanced Range Telemetry (ARTM) Tier-1 Waveforms, which consist of variations of QPSK modulation schemes that encode 2 bits/symbol.

An additional requirement for efficient spectral usage is that the carriers assigned to distinct telemetry signals be spaced as closely as possible. As the carrier spacing is decreased, the spectra of corresponding signals will start overlapping creating ACI which is a limiting factor in carrier spacing assignments. We note that the carrier spacing along with the relative powers of signals in adjacent channels determine the amount of ACI affecting a desired telemetry signal. An illustration of adjacent channel interference and how it might limit channel spacing is illustrated in Figure 1.

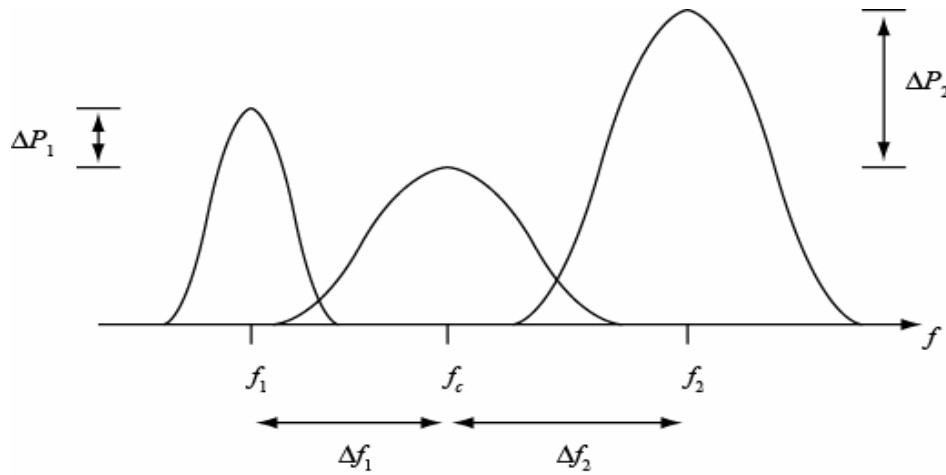


Figure 1: An illustration of adjacent channel interference.

To mitigate the effects of ACI minimum carrier spacings have been recommended for telemetry signals [3]. Recently, the use of interference cancellation techniques has also been investigated as an alternative to enable multiple telemetry signals to be packed more closely together in order to improve the overall efficiency with which the frequency band allocated for telemetry applications is used [4].

Another consequence of the increasing data rates in aeronautical telemetry applications is the fact that the multipath interference affecting propagation of telemetry signals has become more frequency selective as shown by the recently developed channel models for aeronautical telemetry [5]. To mitigate the effects of multipath interference two equalization techniques are investigated in [6]: the constant modulus algorithm (CMA), and the decision-feedback minimum mean square error (DF-MMSE) algorithm.

In our paper we present a new method that is applicable to mitigating both multipath interference and ACI using a linear equalizer based on Kalman filtering theory [7]. We note that Kalman-based equalizers have long been used in communication systems [8], [9]. The paper is organized as follows: we start with a brief description of the ARTM Tier-1 Waveforms used for digital modulation in aeronautical telemetry applications, followed by presentation of the proposed equalizer for ARTM Tier-1 waveforms and numerical results obtained from simulations.

## ARTM TIER-1 WAVEFORMS USED IN AERONAUTICAL TELEMETRY APPLICATIONS

FQPSK modulation [1] is a variant of offset QPSK modulation in which the inphase and quadrature components of the modulated waveforms are cross correlated to produce a signal with quasi-constant envelope. The complex baseband FQPSK waveform is expressed in terms of a set of  $M = 16$  baseband pulses  $S_m(t)$ ,  $m = 0, \dots, M - 1$ , and is represented as

$$f(t) = \sqrt{E_b} \sum_n \left\{ S_{i(n)}(t - nT_s) + jS_{q(n)}[t - (n - 0.5)T_s] \right\} \quad (1)$$

where  $E_b$  represents the average bit energy and  $T_s$  is the symbol duration. During the symbol interval  $nT_s \leq t \leq (n + 1)T_s$  the waveform  $S_{i(n)}(t - nT_s)$  is used to perform amplitude modulation of the inphase component of the carrier, while during the interval  $(n + 0.5)T_s \leq t \leq (n + 1.5)T_s$  the waveform  $S_{q(n)}[t - (n - 0.5)T_s]$  is used to perform amplitude modulation of the quadrature component of the carrier, and indices  $i(n)$ ,  $q(n)$  in  $\{0, \dots, M - 1\}$  are determined by the input data streams as described in [10].

The optimal detector for FQPSK modulation is a sequence detector that uses a trellis which accounts for all possible combinations of waveforms determined by the memory of the waveform mapper [10]. However, in practice a symbol-by-symbol detector as shown in Figure 1 is used. This type of detector can be used also for SOQPSK modulated signals, and its performance is very close to that of the trellis detector.

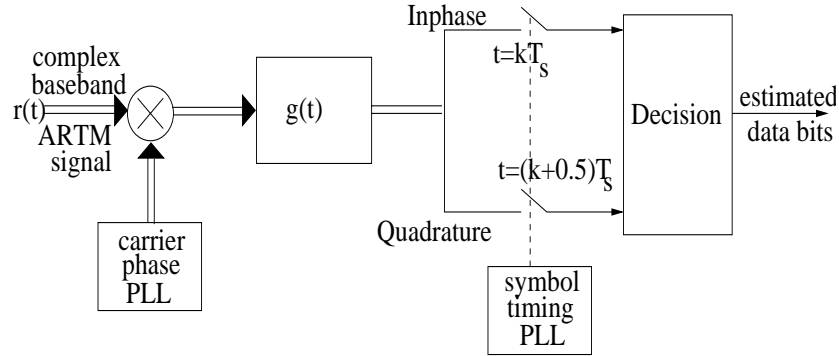


Figure 2: Block diagram of a symbol-by-symbol detector for ARTM Tier-1 Waveforms

SOQPSK modulation [2] is a ternary continuous phase modulation (CPM) scheme with modulation index equal to  $1/2$ , for which the baseband SOQPSK waveform is represented as

$$s(t) = e^{j\phi(t)} \quad (2)$$

with phase  $\phi(t)$  expressed as

$$\phi(t) = \pi \sum_k \alpha(k)g(t - kT_b) \quad (3)$$

where  $\alpha(k)$  in  $\{-1, 0, +1\}$  is the  $k$ -th ternary symbol,  $T_b$  is the bit duration, and  $g(t)$  is a phase pulse that is the time integral of a frequency pulse  $p(t)$  with area equal to  $1/2$ . In our paper we considered the SOQPSK-TG waveforms as defined in [2], for which the frequency pulse is a spectral raised cosine pulse windowed by a temporal raised cosine function that are expressed as

$$g(t) = \int_{-\infty}^t p(x)dx \quad (4)$$

and

$$p(t) = A \frac{\cos\left(\frac{\pi\rho Bt}{2T_b}\right)}{1 - 4\left(\frac{\rho Bt}{2T_b}\right)^2} \times \frac{\sin\left(\frac{\pi Bt}{2T_b}\right)}{\frac{\pi Bt}{2T_b}} \times w_n(t) \quad (5)$$

where the window function is

$$w_n(t) = \begin{cases} 1 & 0 \leq \left|\frac{t}{2T_b}\right| \leq T_1 \\ \frac{1}{2} + \frac{1}{2} \cos\left[\frac{\pi}{T_2}\left(\frac{t}{2T_b} - T_1\right)\right] & T_1 \leq \left|\frac{t}{2T_b}\right| \leq T_2 \\ 0 & T_1 + T_2 < \left|\frac{t}{2T_b}\right| \end{cases} \quad (6)$$

and the constant  $A$  is chosen such that the area of  $p(t)$  is equal to  $1/2$ . The SOQPSK waveform parameters are:  $\rho = 0.7$ ,  $B = 1.25$ ,  $T_1 = 1.5$ , and  $T_2 = 0.5$ . The frequency pulse is defined on the interval  $-2 \leq t/(2T_b) \leq 2$  and spans four signaling intervals, and the mapping from bits to ternary symbols  $\{-1, 0, +1\}$  is done according to [2]. The use of a symbol-by-symbol detector as shown in Figure 1 for more general binary CPM systems was investigated in [11], [12], and for SOQPSK waveforms was discussed in [13].

## THE PROPOSED KALMAN-BASED EQUALIZER FOR ARTM SIGNALS

Let  $r(t)$  be the received baseband signal corresponding to a desired transmitted ARTM signal that employs FQPSK or SOQPSK modulation as described in the previous section, and which is affected by ACI and/or multipath. To mitigate the interference effects on the received signal  $r(t)$  we propose the use of a linear  $N$ -tap delay line filter inspired from the Kalman-filter based channel equalizer proposed by Godard in 1974 [9], that operates on the sampled received baseband ARTM signal  $r(n)$ . We denote the filter tap weights vector by

$$\mathbf{c} = [c_0 \dots c_N]^T \quad (7)$$

with the corresponding tap output vector denoted by

$$\mathbf{r}_n = [r(n) \ r(n-1) \ \dots \ r(n-N)]^\top \quad (8)$$

Then, the equalized signal is expressed as

$$y_n = \mathbf{r}_n^\top \mathbf{c} \quad (9)$$

The values of the equalizer taps are obtained during a training stage in which a set of samples of the desired signal  $\{a_n\}$  known at the receiver is transmitted. The optimal tap values must minimize the expected mean squared distortion  $e_n$  between the training sample and the output of the equalizer, that is

$$\mathcal{E} = E[|\underbrace{a_n - y_n}_{e_n}|^2] = E[|e_n|^2] \quad (10)$$

According to [9] the optimum tap weight vector is given by

$$\mathbf{c}^* = \mathbf{B}^{-1} \mathbf{b} \quad (11)$$

with  $\mathbf{B} = E[\mathbf{r}_n \mathbf{r}_n^\top]$  and  $\mathbf{b} = E[a_n \mathbf{r}_n]$ , and when  $\mathbf{c}$  is chosen to be equal to  $\mathbf{c}^*$  the mean-squared distortion is minimized and equal to  $E^*$ . We note that, even when no noise is present,  $E^* \neq 0$  due to the fact that the equalizer has a finite impulse response, while an infinite impulse response filter is necessary to equalize a finite impulse response channel. We denote by  $e^*(n)$  the distortion when the optimal tap weights are used, and we write the training symbols as

$$a_n = \mathbf{r}_n^\top \mathbf{c}^* + e_n^* \quad (12)$$

with  $E[e_n^{*2}] = E^*$ . With random initialization of the tap weights vector, the dynamic evolution of the optimal tap weights vector  $\mathbf{c}$  during the training stage is described by the following state-space model

$$\begin{aligned} \mathbf{c}_n &= \mathbf{c}_{n-1} \\ a_n &= \mathbf{r}_n^\top \mathbf{c}_n + e_n \end{aligned} \quad (13)$$

in which the state transition matrix is the identity matrix  $\mathbf{I}$ , and the noisy measurement equation expresses the value of training sample  $a_n$  at time instant  $n$  in terms of the actual output of the equalizer  $\mathbf{r}_n^\top \mathbf{c}_n$  at time instant  $n$  and the expected distortion  $e_n$ . The fact that the state transition matrix is equal to the identity matrix implies that at steady state the value of the optimal tap weights vector does not change, and is essentially constant [9].

The optimal tap weights are obtained by applying the Kalman filtering algorithm as in [9], which is different from [8] in which the Kalman filter is actually the equalizer. We recall that, for a general linear system described by the state-space equations

$$\begin{aligned} \mathbf{x}_n &= \mathbf{A}_{n,n-1} \mathbf{x}_{n-1} + \mathbf{w}_n \\ \mathbf{y}_n &= \mathbf{C}_n \mathbf{x}_n + \mathbf{v}_n \end{aligned} \quad (14)$$

where  $\mathbf{x}_n$  is the system state vector,  $\mathbf{A}_{n,n-1}$  is the state transition matrix,  $\mathbf{w}_n$  is the state noise vector with covariance matrix  $\mathbf{Q}_n$ ,  $\mathbf{C}_n$  is the measurement matrix, and  $\mathbf{v}_n$  is the measurement noise vector with covariance matrix  $\mathbf{R}_n$ , the discrete-time Kalman filtering equations [7] for estimation of state vector  $\mathbf{x}$  are:

- 1) predicted state estimate (a priori estimate)

$$\hat{\mathbf{x}}_n^- = \mathbf{A}_{n,n-1} \hat{\mathbf{x}}_{n-1}^+ \quad (15)$$

- 2) predicted measurement equation

$$\hat{y}_n = \mathbf{C}_n \hat{\mathbf{x}}_n^- \quad (16)$$

- 3) error covariance extrapolation

$$\mathbf{P}_n^- = \mathbf{A}_{n,n-1} \mathbf{P}_{n-1}^+ \mathbf{A}_{n,n-1}^\top + \mathbf{Q}_{n-1} \quad (17)$$

- 4) Kalman gain matrix equation

$$\mathbf{K}_n = \mathbf{P}_n^- \mathbf{C}_n^\top (\mathbf{C}_n \mathbf{P}_n^- \mathbf{C}_n^\top + \mathbf{R}_n)^{-1} \quad (18)$$

- 5) error covariance update equation

$$\mathbf{P}_n^+ = (\mathbf{I} - \mathbf{K}_n \mathbf{C}_n^\top)^{-1} \mathbf{P}_n^- \quad (19)$$

- 6) state estimate update (a posteriori estimate)

$$\hat{\mathbf{x}}_n^+ = \hat{\mathbf{x}}_n^- + \mathbf{K}_n (\mathbf{y}_n - \hat{y}_n) \quad (20)$$

For the particular case of the linear system in equation (13) which describes the evolution of the optimal tap weights during the training stage, there is no state noise ( $\mathbf{Q}_n = 0$ ), and the (scalar) measurement noise has variance  $\mathbf{R}_n = E^*$ . The discrete-time Kalman filtering equations (15) – (20) imply that the optimal estimate of the tap weights vector is

$$\begin{aligned} \hat{a}_n &= \mathbf{r}_n^\top \hat{\mathbf{c}}_{n-1} \\ \mathbf{K}_n &= \mathbf{P}_n \mathbf{r}_n (\mathbf{r}_n^\top \mathbf{P}_n \mathbf{r}_n + E^*)^{-1} \\ \mathbf{P}_n &= (\mathbf{I} - \mathbf{K}_n \mathbf{r}_n^\top) \mathbf{P}_{n-1} \\ \hat{\mathbf{c}}_n &= \hat{\mathbf{c}}_{n-1} + \mathbf{K}_n (a_n - \hat{a}_n) \end{aligned} \quad (21)$$

We note that in practice the value of  $E^*$  cannot be known a priori, and in order to compute the Kalman gain  $\mathbf{K}_n$  an estimated value of  $E^*$  is used. According to [9] this has no influence on the successive estimates of the tap weights, and is usually taken between 0.001 and 0.01. After the training stage is completed and steady state is reached, we use the steady state value  $\hat{\mathbf{c}}$  to equalize the received ARTM signal and estimate transmitted symbols using the equalized signal.

## SIMULATION RESULTS

We performed computer simulations to evaluate the improvements in BER when the equalizer filter described in the previous section is used for mitigating multipath interference and ACI in aeronautical telemetry applications using FQPSK and SOQPSK modulation. The data rate for both modulation schemes was taken to be 10 Mbps, with the received signal being sampled at 10 samples/symbol.

For the case of multipath we considered a two-ray propagation channel model which is standard for aeronautical telemetry systems [5], and which was used also in the equalization studies in [6]. We have simulated the system for several values of the ground reflected path gain, and

simulation results are presented in Figure 2 (for FQPSK modulation), respectively Figure 3 (for SOQPSK modulation). The equalizers used 1000 samples for training (corresponding to 100 transmitted symbols), and their lengths for  $\Gamma = 0.3, 0.5, 0.7$  were  $N = 5, 7, 10$  taps respectively for FQPSK signals, and  $N = 3, 5, 7$  taps respectively for SOQPSK signals. In this case we note that the equalizer improves the BER performance by approximately 1 – 5 dB in the case of FQPSK signals, respectively 1 – 3 dB in the case of SOQPSK signals, which is very similar to the performance improvements obtained with the CMA equalizer reported in [6]. We note that performance of the CMA equalizer is heavily dependent on its initialization [14], while that of the proposed Kalman-based equalizer is independent on its initialization [9]. We also note that the performance gains depend on the channel gain value  $\Gamma$ , with smaller improvements for smaller gains, and larger improvements for larger gains.

We have also simulated the use of the proposed Kalman-based equalizer in the presence of ACI, and observed notable performance improvements in the case of FQPSK modulation. Simulation results for FQPSK modulation with two ACI signals (one on each side of the desired signal, with the same power as the desired signal) for various carrier spacing values and no multipath are presented in Figure 4, and with the same two ACI signals but with multipath with  $\Gamma = 0.3$  are presented in Figure 5. In both cases a  $N = 5$  tap equalizer filter with 1000 samples for training (corresponding to 100 transmitted symbols) yielded the best performance improvement, and we note that in this case the Kalman-based equalizer filter provides performance very close to that when no ACI is present. We also note that all ACI signals were assumed synchronized with the desired signal, and that there is about 1 dB loss in performance when synchronization is no longer assumed. In the case of SOQPSK modulation however, the proposed Kalman-based equalizer didn't yield significant improvements.

## CONCLUSIONS

In this paper we presented a new method for mitigating ACI and multipath interference in aeronautical telemetry applications using ARTM Tier-1 waveforms. The proposed method uses a linear filter which has been used for channel equalization for high-speed communication systems and which is obtained by applying Kalman filtering techniques, and improves BER performance in the presence of multipath. In addition, in the case of FQPSK modulation it can also be used for ACI mitigation.

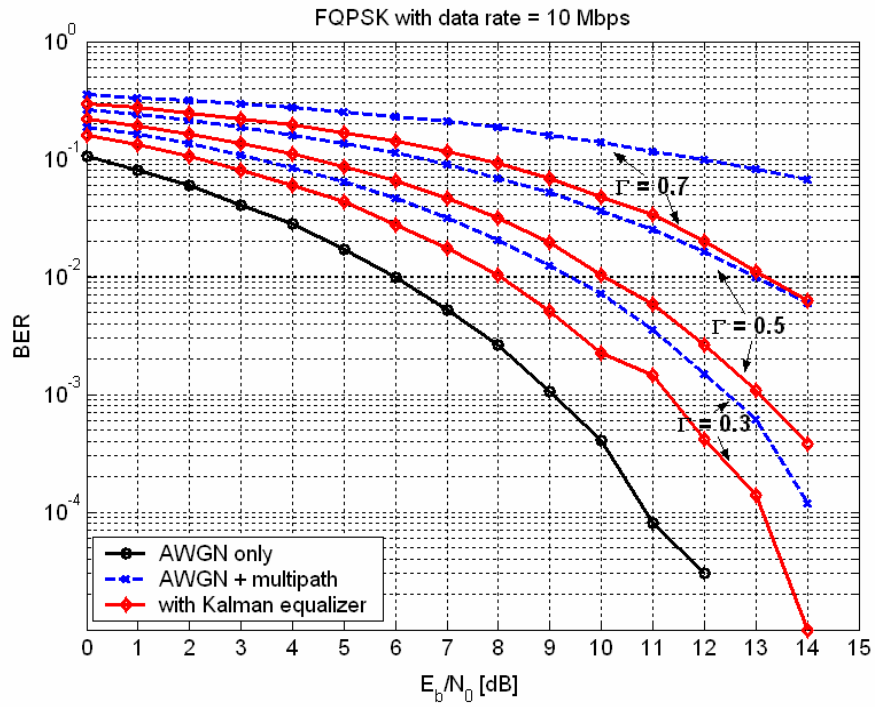


Figure 3: BER performance for FQPSK signals with multipath channel.

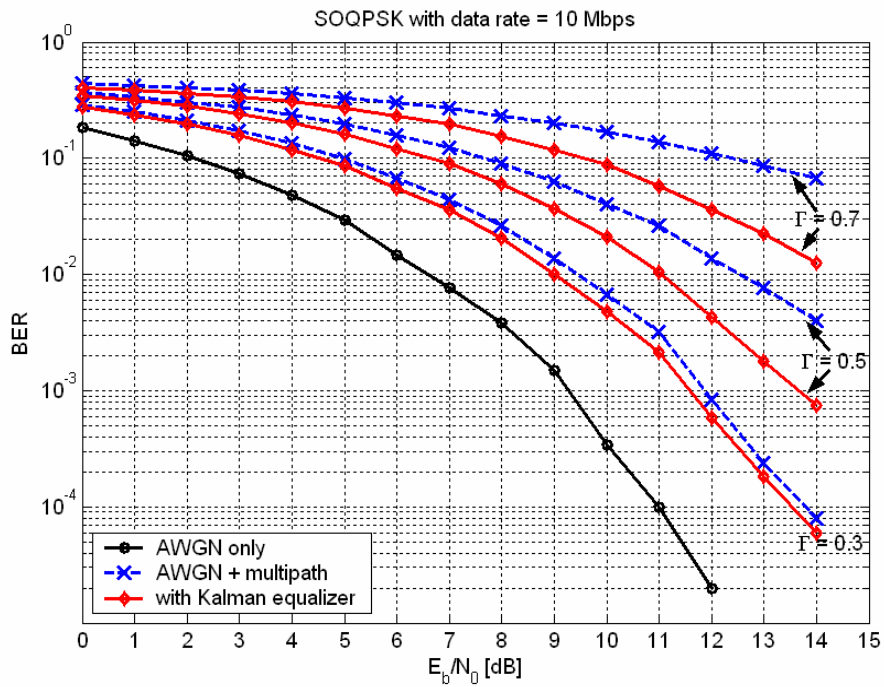


Figure 4: BER performance for SOQPSK signals with multipath channel.



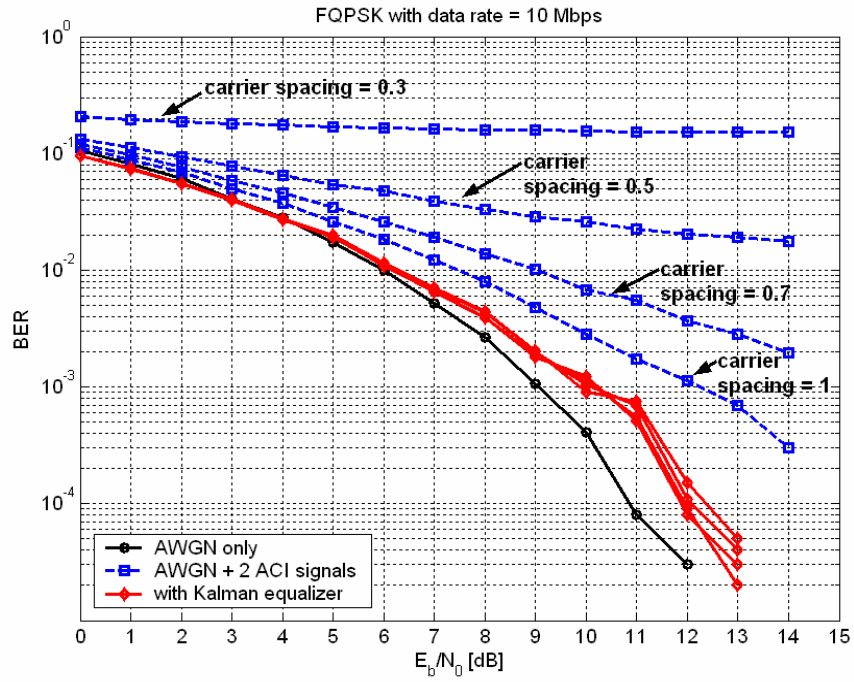


Figure 4: BER performance for FQPSK signals with 2 ACI signals

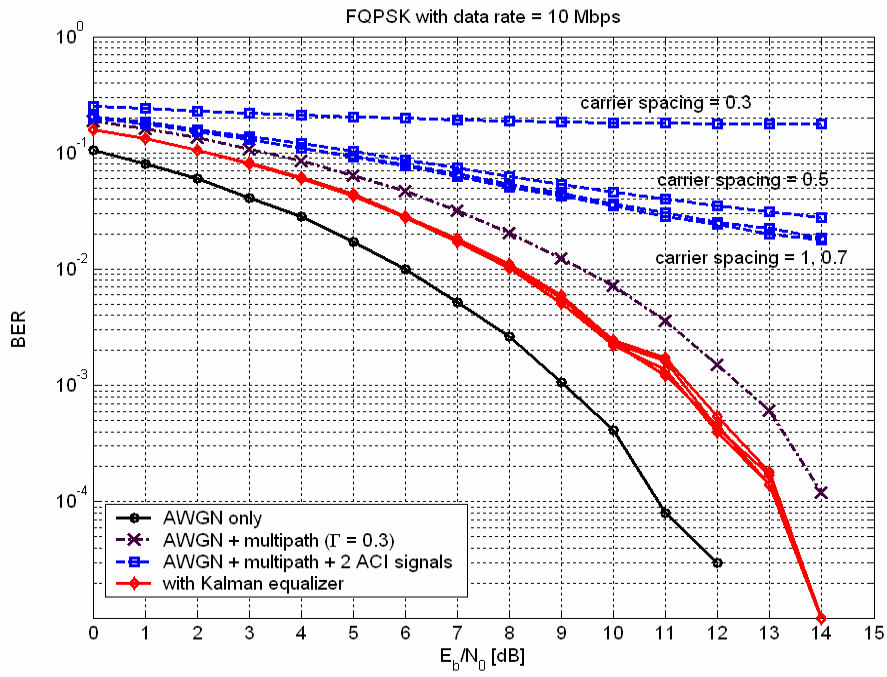


Figure 5: BER performance for FQPSK signals with 2 ACI signals and multipath

## REFERENCES

- [1] W. Gao and K. Feher, "FQPSK: A Bandwidth and RF Power Efficient Technology for Telemetry Applications," in *Proceedings International Telemetry Conference*, Las Vegas, NV, October 1997, pp. 480–488.
- [2] T. Hill, "An Enhanced, Constant Envelope, Interoperable Shaped Offset QPSK (SOQPSK) Waveform for Improved Spectral Efficiency," in *Proceedings International Telemetry Conference*, San Diego, CA, October 2000, pp. 90–96.
- [3] E. Law, "Recommended Minimum Telemetry Frequency Spacing with CPAFASK, CPM, SOQPSK, and FQPSK Signals," in *Proceedings International Telemetry Conference*, San Diego, CA, October 2003, pp. 942–950.
- [4] T. M. Ali, M. Saquib, and M. Rice, "Interference Cancellation Using ARTM Tier-1 Waveforms in Aeronautical Telemetry," in *Proceedings International Telemetry Conference*, Las Vegas, NV, October 2005, pp. 111–121.
- [5] M. Rice, A. Davis, and C. Bettweiser, "Wideband Channel Model for Aeronautical Telemetry," *IEEE Transactions on Aerospace and Electronic Systems*, vol. 40, no. 1, pp. 57–69, January 2004.
- [6] M. Rice and E. Satorius, "Equalization Techniques for Multipath Mitigation in Aeronautical Telemetry," in *Proceedings 2004 IEEE Military Communications Conference – MILCOM'04*, vol. 1, Monterey, CA, November 2004, pp. 65–70.
- [7] R. E. Kalman, "A New Approach to Linear Prediction and Filtering Theory," *Journal of Basic Engineering, Transactions of ASME*, no. 81, pp. 35–45, 1960.
- [8] R. E. Lawrence and H. Kaufman, "The Kalman Filter for the Equalization of a Digital Communications Channel," *IEEE Transactions on Communications*, vol. COM-19, no. 6, pp. 1137–1141, December 1971.
- [9] D. Godard, "Channel Equalization Using a Kalman Filter for Fast Data Transmission," *IBM Journal of Research Development*, vol. 18, no. 3, pp. 267–273, May 1974.
- [10] M. Simon, *Bandwidth-Efficient Digital Modulation with Application to Deep Space Communications*. Wiley-Interscience, 2003.
- [11] A. Svensson and C.-E. Sundberg, "Optimum MSK-Type Receivers for CPM on Gaussian and Rayleigh Fading Channels," *IEE Proceedings*, pp. 480–490, August 1984.
- [12] A. Svensson and C.-E. Sundberg, "Serial MSK-Type Detection of Partial Response Continuous Phase Modulation," *IEEE Transactions on Communications*, vol. 33, no. 1, pp. 44–52, January 1985.
- [13] M. Geoghegan, "Optimal Linear Detection of SOQPSK," in *Proc. Int. Telemetry Conf.*, San Diego, CA, October 2002.
- [14] C. R. Johnson Jr., P. Schniter, T. J. Endres, J. D. Behm, D. R. Brown, and R. A. Casas, "Blind Equalization Using the Constant Modulus Criterion: A Review," *Proceedings of the IEEE*, vol. 86, no. 10, pp. 1927–1950, October 1998.